Acta Pharmacologica Sinica (2018) 39: 930–941

www.nature.com/aps

Article

Chinese herbal formula Fuzheng Huayu alleviates CCl_4-induced liver fibrosis in rats: a transcriptomic and proteomic analysis

Shu DONG[1, #], Fei-fei CAI[1, #], Qi-long CHEN[1], Ya-nan SONG[1], Yang SUN[1], Bin WEI[1], Xiao-yan LI[1], Yi-yang HU[2], Ping LIU[3, *], Shi-bing SU[1, *]

[1]Research Center for Traditional Chinese Medicine Complexity System, Shanghai University of Traditional Chinese Medicine, Shanghai 201203, China; [2]Institute of Liver Diseases, Shuguang Hospital Affiliated to Shanghai University of Traditional Chinese Medicine, Shanghai 201203, China; [3]Institute of E, Shanghai University of Traditional Chinese Medicine, Shanghai 201203, China

Abstract

Liver fibrosis is a consequence of chronic liver disease that can progress to liver cirrhosis or even hepatocarcinoma. Fuzheng Huayu (FZHY), a Chinese herbal formula, has been shown to exert anti-fibrotic effects. To better understand the molecular mechanisms underlying the anti-fibrotic effects of FZHY, we analyzed transcriptomic and proteomic combination profiles in CCl_4-induced liver fibrosis in rats, which were treated with extracted FZHY powder (0.35 $g{\cdot}kg^{-1}{\cdot}d^{-1}$, ig) for 3 weeks. We showed that FZHY administration significantly improved liver function, alleviated hepatic inflammatory and fibrotic changes, and decreased the hydroxyproline content in the livers of CCl_4-treated rats. When their liver tissues were examined using microarray and iTRAQ, we found 255 differentially expressed genes (fold change ≥1.5, $P<0.05$) and 499 differentially expressed proteins (fold change ≥1.2, $P<0.05$) in the FZHY and model groups. Functional annotation with DAVID (The Database for Annotation, Visualization and Integrated Discovery) showed that 15 enriched gene ontology terms, including drug metabolic process, response to extracellular stimulus, response to vitamins, arachidonic acid metabolic process, response to wounding, and oxidation reduction might be involved in the anti-fibrotic effects of FZHY; whereas KEGG pathway analysis revealed that eight enriched pathways, including arachidonic acid metabolism, retinol metabolism, metabolism of xenobiotics by cytochrome P450, and drug metabolism might also be involved. Moreover, the protein-protein interaction network demonstrated that 10 core genes/proteins overlapped, with Ugt2a3, Cyp2b1 and Cyp3a18 in retinol metabolism pathway overlapped to a higher degree. Compared to the model rats, the livers of FZHY-treated rats had significantly higher mRNA and protein expression levels of Ugt2a3, Cyp2b1 and Cyp3a18. Furthermore, the concentration of retinoic acid was significantly higher in the FZHY-treated rats compared with the model rats. The results suggest that the anti-fibrotic effects of FZHY emerge through multiple targets, multiple functions, and multiple pathways, including FZHY-regulated retinol metabolism, xenobiotic metabolism by cytochrome P450, and drug metabolism through up-regulated Ugt2a3, Cyp2b1, and Cyp3a18. These genes may play important anti-fibrotic roles in FZHY-treated rats.

Keywords: Chinese herbal formula; Fuzheng Huayu; CCl_4-induced liver fibrosis; transcriptomics; proteomics

Acta Pharmacologica Sinica (2018) 39: 930–941; doi: 10.1038/aps.2017.150; published online 2 Nov 2017

Introduction

Hepatic fibrosis, a wound-healing response to various chronic stimuli including hepatic viral infection, metabolic disorders, alcohol abuse, and autoimmune disease in the liver[1], is characterized by the excessive accumulation of extracellular matrix (ECM) proteins and collagen[2]. Hepatic fibrosis commonly develops due to chronic inflammation and the persistence of this inflammation has been associated with progressive hepatic fibrosis[3]. Furthermore, the fibrosis can progress to liver cirrhosis, ultimately leading to organ failure and death[4]. Therefore, it is important to effectively reverse liver fibrosis. Western medicine lacks targeted drugs that can reverse liver fibrosis and repair injured livers in any meaningful way[5], but traditional Chinese medicine (TCM) treatment strategies have been developed after the elucidation of the underlying mechanisms of liver fibrosis.

Among many TCMs, the Fuzheng Huayu (FZHY) formula, also called TCM 319, is an SFDA-approved, effective, anti-

# These authors contributed equally to this work.
*To whom correspondence should be addressed.
E-mail shibingsu07@163.com (Shi-bing SU);
liuliver@vip.sina.com (Ping LIU)
Received 2017-03-16 Accepted 2017-08-13

fibrotic medicine[6]. Animal experiments indicated that FZHY can effectively improve liver fibrosis and inflammation[7] and a meta-analysis indicated that FZHY could effectively improve liver function, alleviate hepatic fibrosis, decrease Child-Pugh scores, and relieve symptoms caused by liver dysfunction[8]. The mechanisms underlying FZHY effects is primarily related to suppression of the pathways involved in autocrine activation in hepatic stellate cells (HSCs) and fibrotic liver tissue and regulation of the expression of related cytokines, such as VEGF[9], TGF-β1[10], p38 mitogen-activated protein kinase (MAPK), stress-activated protein kinase, and Jun N-terminal kinase (SAPK/JNK)[11]. Due to the complexity of the Chinese herbal formula (CHF), which is a mixture of multiple compounds based on TCM theory, systematically exploring the molecular mechanisms and identifying potential targets and their actions remain challenging in FZHY research.

The development of system biology and network pharmacology has provided an expanded opportunity for CHF research, which can be used to understand the scientific basis of CHF at the molecular level from a system perspective[12]. As an integrated multidisciplinary concept, network pharmacology, which is based on high throughput data such as transcriptomics and proteomics, affords a novel network mode that turns the idea of "one gene, one target" into "multiple targets and multiple effects"[13]. Recently, high throughput biological data have been widely used in CHF research to aid in the exploration of CHF targets and the elucidation of potential mechanisms of action[14]. Previous studies on CHFs[15], including QiShenYiQi[16], Zhi-Zi-Da-Huang Decoction[17], and HuangQi Decoction[18, 19], have received attention for their investigations of pharmacological mechanisms of action using network pharmacology. This provides an approach for further investigation into the molecular mechanisms underlying the effects of FZHY against fibrosis, which may fill a gap in system biology-related research.

In the present study, we performed an integrative analysis with mRNA microarray and iTRAQ data to evaluate key targets and the significance of alterations of biological functions and associated pathways that may be involved in the molecular mechanisms of the anti-fibrotic effects of FZHY. In addition, we verified the validity of the predicted FZHY targets that may regulate the associated pathways.

Material and methods

Drugs, chemicals, and animal administration

Wistar rats (150–160 g) were purchased from the Shanghai Laboratory Animal Center of the Chinese Academy of Sciences (Shanghai, China). Carbon tetrachloride (CCl_4) (batch number: 20070721) and olive oil (batch number: 060312) were purchased from Sinopharm Co, Ltd (Shanghai, China). FZHY formula (capsule, batch number: 070906) was purchased from Shanghai HuangHai pharmaceutical Co, Ltd (Shanghai, China) and is composed of 8 g of *Salvia miltiorrhiza*, 4 g of *Cordyceps sinensis*, 2 g of peach kernel, 2 g of pollen pini, 6 g of *Gynostemma pentaphylla*, and 2 g of *Schisandra*.

The rats were acclimated to the laboratory conditions for seven days and then randomly allocated to two groups: the control group (normal group, n=6) and the CCl_4-treated group (model group, n=20). Rats in the control group were conventionally raised and those in the model group were intraperitoneally injected with 50% CCl_4 in olive oil solution at 1 mL/kg bodyweight twice weekly for nine weeks[20]. At the seventh week, the rats in the CCl_4-treated group were randomly divided into two groups: the model group (n=10) and the FZHY-treated group (n=10). The daily dose of FZHY for human adults weighing 70 kg is 24 g (according to the clinical dosage) and the powder paste rate of FZHY used in this study is 0.1359 (according to the preparation and extraction process), so the rats were gavaged using extracted FZHY powder (method of decocting) at a dosage of 0.35 g/kg/d for three weeks. Rats in the model group were administered the corresponding amount of saline. The animal room was maintained at a temperature of 22 °C to 26 °C with a relative humidity of 40% to 70%. According to related studies[21, 22], rules of animal experimentation[23], and the guide for animal care and use, the rat weight was used to assess the health and welfare of the animals once every two weeks. When weight loss was 20%–30% of the average weight of the control group, the animals in model group were euthanized by cervical dislocation prior to the end of the study. All experiments in this study were approved by the Animal Ethics Committee of Shanghai University of Traditional Chinese Medicine and performed in accordance with the Guide for Animal Care and Use.

Sample preparation and evaluation of the systemic protection induced by FZHY treatment

After nine weeks, the animals were fasted overnight and anesthetized with 20% urethane by intraperitoneal injection, 1–1.5 g/kg, after being weighed according to the rules of animal ethics and experiments[24, 25]. Blood was collected from the abdominal aorta. For the liver function evaluation, aspartate aminotransferase (AST) and alanine aminotransferase (ALT) were determined with biochemical kits (Nanjing Jiancheng Biological Engineering Research Institute, Nanjing, China) following the manufacturer's instructions. To further evaluate the anti-inflammatory effects of FZHY, proinflammatory cytokines, interleukin-6 (IL-6) and tumor necrosis factor α (TNF-α) were detected with ELISA kits (MultiSciences (Lianke) Biotech Co, Ltd, Hangzhou, China) following the manufacturer's instructions. Superoxide Dismutase (SOD) and Malondialdehyde (MDA) were detected to evaluate the effect of FZHY against oxidative stress. The experiments were performed with biochemical kits (Nanjing Jiancheng Biological Engineering Research Institute, Nanjing, China) following the manufacturer's instructions.

After euthanization, liver tissues were collected, weighed, cut into small pieces, and then fixed in 4% paraformaldehyde phosphate buffer and subjected to paraffin embedding for hematoxylin and eosin (H&E) staining and Sirius Red staining. Furthermore, to evaluate the degree of liver fibrosis, we evaluated the hydroxyproline (Hyp) content in liver tissue with a Hyp-detection kit (Nanjing Jiancheng) following the manufac-

turer's instructions. The remaining liver tissues were frozen in liquid nitrogen and preserved at –80 °C for proteome analysis and mRNA microarray assays.

Total RNA extractions and mRNA microarrays

Total RNA in liver tissue samples from the normal group (n=3), model group (n=3), and FZHY-treated group (n=3) was isolated using TRIzol Reagent (Cat# 15596-018, Life Technologies, Carlsbad, CA, USA) following the manufacturer's instructions and checked for an RNA integrity number (RIN) to inspect RNA integration using an Agilent Bioanalyzer 2100 (Agilent Technologies, Santa Clara, CA, USA). Qualified total RNA was further purified using an RNeasy Mini Kit (Cat# 74106, QIAGEN, GmBH, Germany) and an RNase-Free DNase Set (Cat# 79254, QIAGEN) and stored at –80 °C. Quality control was carried out using the RIN number obtained from the Agilent Bioanalyzer 2100 (Agilent Technologies). An mRNA microarray analysis was conducted on each total RNA sample using a Low Input Quick Amp Labeling Kit, One-Color (Cat# 5190-2305, Agilent Technologies) and a Gene Expression Hybridization Kit (Cat# 5188-5242, Agilent Technologies) following the manufacturer's protocol. Slides were scanned using an Agilent Microarray Scanner (Cat# G2565CA, Agilent Technologies) with the default settings. Feature Extraction software 10.7 (Agilent Technologies) was used to evaluate the raw data and the data were normalized using the Quantile algorithm, Gene Spring Software 11.0 (Agilent Technologies).

iTRAQ sample preparation and quantification

Frozen samples (same with extracted RNA) were ground to a fine powder in liquid nitrogen and suspended in STD buffer (4% SDS, 1 mmol/L DTT, 150 mmol/L TrisHCl, pH 8.0). The suspension was vortexed and incubated in boiling water for 5 min. The supernatant was obtained by centrifugation after ultrasonication. The protein concentration of each sample was determined using 2D Quantification Kit (GE Healthcare, Buckinghamshire, UK). A total of 100 μg of each sample was denatured, reduced, and alkylated as described in the iTRAQ protocol (Applied Biosystems, Foster City, CA, USA). Each sample was digested overnight with 0.1 μg/μL trypsin solution at 37 °C. The digested peptides were dried by vacuum centrifugation.

All samples were labeled according to the manufacturer's protocol (Applied Biosystems). The nine samples were pooled and vacuum-dried. The pooled sample was separated on a Poly-LC strong cation exchange column (4.6 mm×100 mm) using a Nano HPLC System (GE Healthcare). Subsequently, the fractionated samples were analyzed by LC-MS/MS based on a Q-Exactive mass spectrometer (Thermo Finnigan, CA, USA).

For peptide data analysis, raw mass data was processed using Proteomics Tools (Abcam, Cambridge, UK) and normalized according to signal values. Proteins were identified with MASCOT software (Matrix Science, Boston, MA, USA). The following filters were used in this study: protein False Discovery Rate (FDR) ≤0.01; and peptide FDR ≤0.01.

Data analysis

Transcriptomics and proteomics data were first analyzed using SAS online software. A |fold change| >1.5 and P-values <0.05 were used to classify differentially expressed genes (DEGs) and a |fold change| >1.2 was used to classify differentially expressed proteins (DEPs). Gene ontology (GO) and pathway analyses with the DEGs and DEPs was performed using DAVID online and the parameters were set as follows: count=2, ease=0.05. An integrative analysis of the DEGs and DEPs was performed using a Venn analysis. A protein-protein interaction (PPI) network was constructed using STRING online analysis and Cytoscape version 3.2.0. The co-expressed genes among the overlapped DEGs and DEPs with the greatest degree of overlap were presumed to be the core genes and were considered to be potential targets and to play important roles in the mechanisms underlying the anti-fibrotic effects of FZHY.

Continuous data were calculated using the homogeneity test of variance and then a one-way ANOVA (Homogeneity of variance) or non-parametric test (Heterogeneity of variance) was performed. Differences for each parameter were evaluated and considered significant if P-values were less than 0.05.

Quantitative RT-PCR

The extracted 2 μg of total RNA was used for reverse transcription (RT) to generate template cDNA. The relative mRNA levels were determined by quantitative PCR. Since the expression of PPIA was more stable in all samples than the expression of GAPDH, PPIA served as an internal reference gene. The PCR parameters were as follows: 95 °C for 1 min, followed by 40 cycles of denaturation at 95 °C for 15 s, annealing at 60 °C for 15 s, and extending at 72 °C for 45 s. The primer sequences were designed using Primer 5.0 and were searched for specificity using NCBI-Blast. The primer sequences were as follows (Table 1). And the quantitative PCR results were calculated

Table 1. Primer sequences.

Gene	Primer sequence
α-SMA	(F) 5'-CATCACCAACTGGGACGACA-3'
	(R) 5'-TCCGTTAGCAAGGTCGGATG-3'
Collagen I	(F) 5'-GACTGTCCCAACCCCCAAAA-3'
	(R) 5'-CTTGGGTCCCTCGACTCCTA-3'
Fibronectin	(F) 5'-GGCTACATCATCCGCCATCA-3'
	(R) 5'-GCCCGGATTAAGGTTGGTGA-3'
Ugt2a3	(F) 5'-TAGTGTTTTCGCTGGGGTCA-3'
	(R) 5'-TCTGGGCAAGGGCTGATG-3'
Cyp2b1	(F) 5'-TCATCGACACTTACCTTCTGC-3'
	(R) 5'-GTGTATGGCATTTTACTGCGG-3'
Cyp3a18	(F) 5'-ATCCCTTCGTGCAGAAAGCC-3'
	(R) 5'-CTTTTGCACATTGGGGCGAG-3'
PPIA	(F) 5'-CCAAACACAAATGGTTCCCAGT-3'
	(R) 5'-ATTCCTGGACCCAAAACGCT-3'
β-Actin	(F) 5'-ACGTTGACATCCGTA-3'
	(R) 5'-CTGGAAGGTGGACAGTGAG-3'

using the $2^{-\Delta\Delta Ct}$ method.

Western blot

Liver tissue homogenates were sonicated for complete dissolution and centrifuged at 12 000 revolutions per minute for 30 min at 4 °C to separate the membrane-containing fraction (pellet) from the cytosol. Proteins (100 μg) were separated by 10% SDS-polyacrylamide gel electrophoresis. The separated proteins were blotted onto a nitrocellulose membrane (NC membrane, Millipore, Massachusetts, USA) and the membrane was washed for 10 min with TBST and then immersed in blocking buffer containing 5% nonfat dry milk in TBST for 1 h at room temperature. The blot was washed again with TBST and incubated overnight at 4 °C with the polyclonal primary antibodies Ugt2a3 and Cyp2b1 (Santa Cruz Biotechnology, Inc, CA, USA) diluted 1:500 in 5% nonfat dry milk and Cyp3a18 (Shanghai-Youke Biotechnology, Inc, Shanghai, China) diluted 1:1000 in 5% nonfat dry milk. The blot was then incubated with secondary antibody (Cell Signaling Technology, Danvers, MA, USA) for 1 h at room temperature and scanned by infrared rays with an Odyssey Infrared Imager (LI-COR, NE, USA). The bands were quantified by densitometry using Odyssey software (version 1.2, LI-COR).

ELISA

Liver tissue homogenates were sonicated for complete dissolution and centrifuged at 12 000 revolutions per minute for 5 min at 4 °C to obtain the supernatant, which was used to test the concentration of retinoic acid. The experiments were performed using an ELISA Kit according to the manufacturer's protocol (ml0202932, Shanghai Enzyme-linked Biotechnology Co, Ltd, Shanghai, China).

Results

FZHY attenuates inflammatory lesions and liver fibrosis in rats

In this study, we regularly observed the rats in the normal, model, and FZHY-treated groups. The rats in the model group had lower body weights. Compared with the model group, the rats in the FZHY-treated group had higher body weights (Figure 1). In this study, no animals met our humane endpoint before euthanasia or death without anesthetization. Blood biochemistry evaluations, including ALT and AST, were performed to evaluate liver function. As shown in Figure 2A, while the levels of ALT and AST increased significantly in the model group compared to the normal group (P<0.01), there were significantly lower levels of ALT and AST in the FZHY-treated group compared to the model group (P<0.01). TNF-α and IL-6 were also evaluated and the results showed that they were much lower in the FZHY-treated group (P<0.05), indicating that FZHY treatment could attenuate liver inflammation in the model rats.

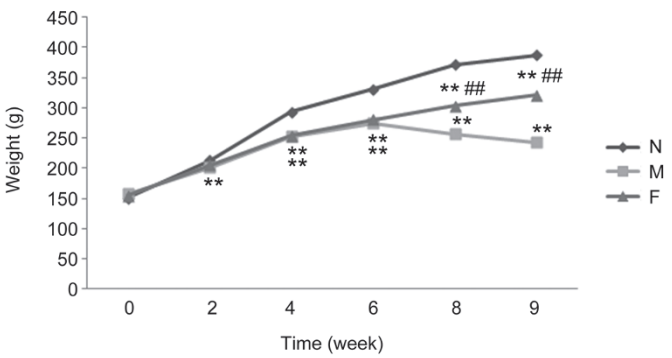

Figure 1. Weight curves of the rats in the normal, model, and FZHY-treated groups. N, normal group (n=6); M, model group (n=10); F, FZHY-treated group (n=10). $^{**}P$<0.01 compared with the normal group; $^{\#\#}P$<0.01 compared with the model group.

The effect of FZHY against oxidative stress was evaluated with SOD and MDA. There were no statistically significant differences between the groups (Figure 2B).

In addition, histopathological examinations, detection of the Hyp content and the expression of fibrosis-related genes including αSMA, collagen I and fibronectin in rat liver tissues were performed to evaluate the degree of liver fibrosis. H&E staining in the normal group showed that the hepatic lobule structure was clear and without inflammatory cells. After nine weeks of CCl_4-administration, there was moderate inflammatory cell infiltration around edematous liver cells in the model group. In the FZHY-treated group, only mild pathological changes and few inflammatory cells were observed (Figure 3A). Sirius Red staining indicated no fibrosis in the normal group, but in the model group, the structure of the hepatic lobule was destroyed by paraplastic connective tissue and mild to serious fibrosis was detected. In the FZHY-treated group, there were few fibrous septa in the liver tissue (Figure 3B). Hyp content detection was performed to evaluate the degree of liver fibrosis. Hyp contents in liver tissue were significantly increased in the model group compared to the normal group, but the FZHY group displayed significantly decreased levels of Hyp contents compared to the model group (P<0.01, Figure 2C). The gene expression levels of αSMA, collagen I and fibronectin in liver tissues were significantly increased in the model group compared to the normal group, but in the FZHY group, the expression levels were decreased compared to the model group to a certain extent (Figure 2C). These results indicated that FZHY treatment attenuated inflammatory lesions and liver fibrosis in rats.

DEGs and DEPs in the FZHY-treated group

In this study, DEGs were screened with fold changes ≥1.5 and P-values ≤0.05. In total, 255 genes were differentially expressed. Of these, 122 genes were down-regulated and 133 were up-regulated in the liver tissues of the FZHY-treated group (n=3). Figure 4A shows the top 10 DEGs that were both up- and down-regulated. DEPs were screened with fold changes ≥1.2. In total, 499 proteins were differentially expressed. Of these, 247 genes were down-regulated and 260 were up-regulated. Figure 4B shows the top 10 DEPs that were both up- and down-regulated. We found that 18 DEGs and DEPs overlapped by Wayne analysis using transcrip-

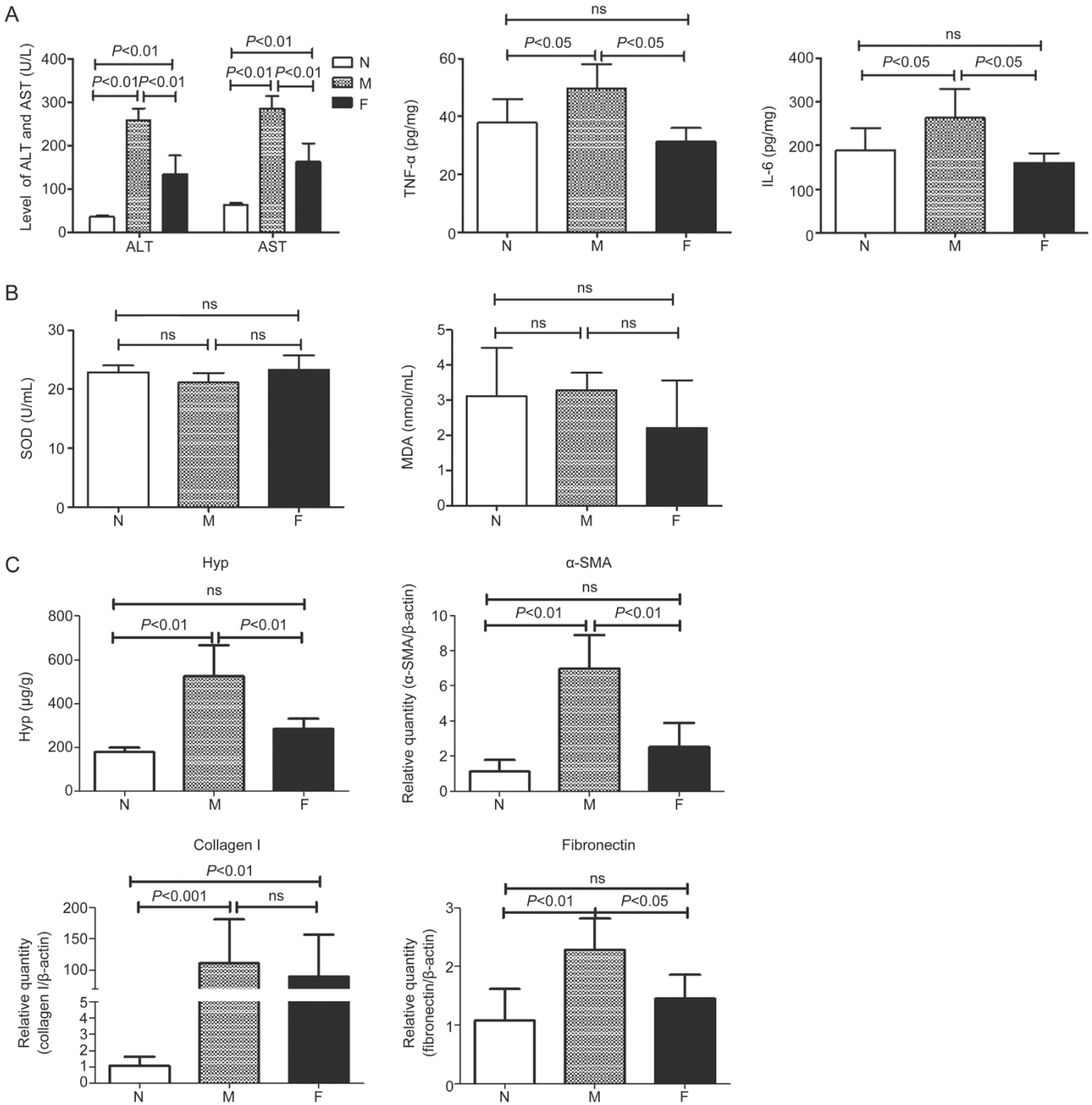

Figure 2. Evaluation of the effect of FZHY against inflammation, oxidative stress and fibrosis. (A) the levels of ALT, AST, TNF-α and IL-6; (B) the levels of SOD and MDA; (C) the levels of Hyp, α-SMA, collagen I and fibronectin in liver tissues. N, normal group (*n*=6); M, model group (*n*=10); F, FZHY-treated group (*n*=10).

tomics and proteomics data (Figure 4C), including Kpna4, Kng1l1, Kng1, Fgg, Fgb, LOC500956, Fbln1, Eef1e1, Me1, Sds, Ugt2b37, Ugt2a3, Cyp2b1, Ugt2b1, LOC259245, Cyp3a18, Obp3, and Cyp3a23/3a1.

Mechanisms underlying the anti-fibrotic effects of FZHY by the GO and pathway analyses

GO and pathway analyses were performed to evaluate the main mechanisms underlying the anti-fibrotic effects of FZHY. The results indicated that 255 DEGs were enriched in 55 GO terms, including drug metabolic process, oxidation reduction, response to wounding, arachidonic acid metabolic process, response to extracellular stimulus, ER-nuclear sterol response pathway, and response to endogenous stimulus were enriched in 10 pathways, including metabolism of xenobiotics by cytochrome P450, drug metabolism, retinol metabolism, steroid

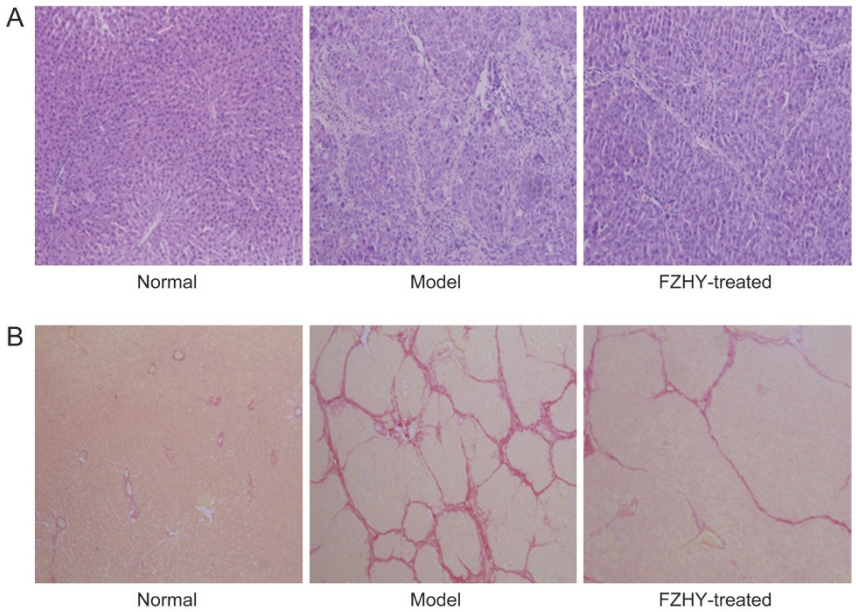

Figure 3. Histopathological examination in the normal, model, and FZHY-treated groups. (A) H&E staining (10×20); (B) Sirius Red stain (10×10).

hormone biosynthesis, pentose and glucuronate interconversions, starch and sucrose metabolism, complement and coagulation cascades, arachidonic acid metabolism, and ascorbate and aldarate metabolism.

In total, 499 DEPs were enriched in 126 GO terms, including oxidation reduction, response to drug, response to endogenous stimulus, arachidonic acid metabolic process, response to extracellular stimulus, fatty acid metabolic process, response to wounding, response to oxidative stress, inflammatory response, and ECM organization were enriched in 20 pathways, including drug metabolism, metabolism of xenobiotics by cytochrome P450, retinol metabolism, arachidonic acid metabolism, PPAR signaling pathway, vascular smooth muscle contraction, fatty acid metabolism, ECM-receptor interaction, and focal adhesion. As shown in Figure 5A and 5B, 15 common GO terms and eight pathways were overlapped in the FZHY-treated group, including response to extracellular stimulus, oxidation reduction, retinol metabolism, metabolism of xenobiotics by cytochrome P450, and drug metabolism pathways. This suggests that the mechanisms underlying the anti-fibrotic effects of FZHY is multi-functional and involves multiple pathways.

Potential targets of FZHY and its regulated pathways

Based on the DEGs and DEPs common to the FZHY and the model groups, a PPI network was constructed using STRING 9.1. The network was analyzed with Cytoscape 3.2.0. The degrees of the nodes were calculated to screen the hub proteins/genes that may play important roles in the FZHY treatment of liver fibrosis. Moreover, there were 10 nodes of overlapped DEG and DEP co-expression in this PPI network (Figure 6), including Kng1l1, Kng1, Fgg, Fgb, Fbln1, Eef1e1, Me1, Ugt2a3, Cyp2b1, and Cyp3a18. Among these, Ugt2a3, Cyp2b1, and Cyp3a18 overlapped to a higher degree (Figure 6), indicating that they may be the targets involved in the mechanisms underlying the anti-fibrotic effects of FZHY. Furthermore, the pathway analysis showed that these proteins were enriched in retinol metabolism, metabolism of xenobiotics by cytochrome P450, and drug metabolism pathways. Figure 7 shows that FZHY regulated retinol metabolism through up-regulated Ugt2a3, Cyp2b1, and Cyp3a18.

Validation of potential targets with qRT-PCR and Western blot

According to the above analysis, Ugt2a3, Cyp2b1, and Cyp3a18 were not only overlapped DEGs and DEPs in the integrative analysis of transcriptomics and proteomics data but also overlapped in their co-expression in the PPI network. Therefore, they were identified as potential targets and further evaluated by Western blot analysis and qRT-PCR. The evaluation with qRT-PCR was carried out using a cohort of independent samples from the model (n=9) and FZHY (n=8) groups. The expression levels of Ugt2a3, Cyp2b1, and Cyp3a18 were consistent with the results from the microarrays. At the transcript expression level, statistical significance was noted for Ugt2a3 (P=0.017), Cyp2b1 (P=0.021), and Cyp3a18 (P=0.043) (Figure 8A–8C). Transcript levels were significantly elevated in the FZHY group compared to the model group. In addition, Western blot was carried out using the same samples. The expression levels of Cyp2b1 and Cyp3a18 were consistent with the results from the iTRAQ data. At the protein expression level, Cyp2b1 (P=0.019) and Cyp3a18 (P=0.027) (Figure 8D, 8E) were significantly elevated in the FZHY group compared to the model group. Due to a problem with the Ugt2a3 antibody, there were no bands for Ugt2a3 expression.

Concentration of retinoic acid with ELISA

To further demonstrate our findings and clarify that the potential targets had important effects in mediating the retinol

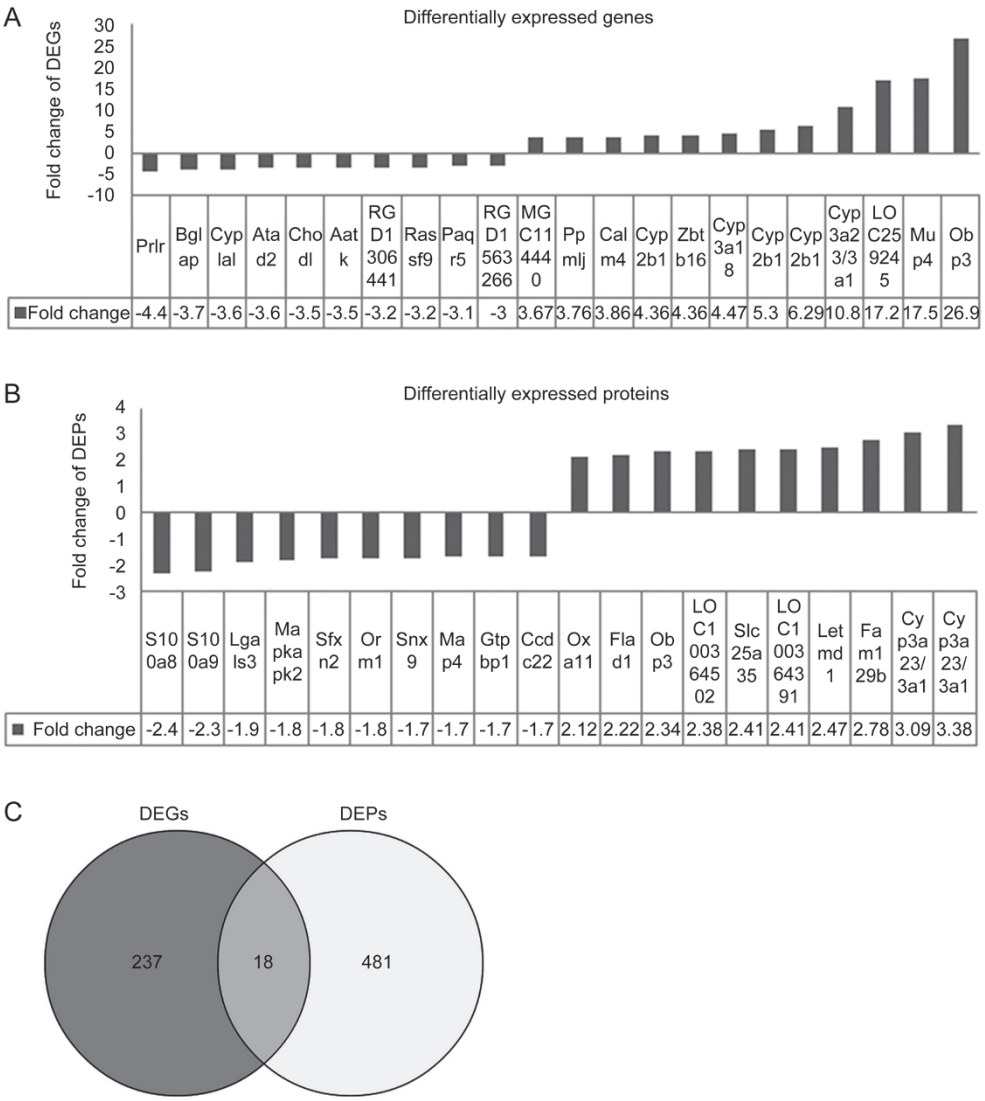

Figure 4. Top 10 up- and down-regulated DEGs and DEPs and overlapped DEGs and DEPs between the FZHY group and the model group. (A) DEGs; (B) DEPs; (C) overlapped DEGs and DEPs by Wayne analysis. Dark part, DEGs; light part, DEPs; middle part, overlapped DEGs and DEPs.

metabolic pathway, we also screened other related genes in the retinol metabolic pathway, such as ADHs and Radh1/2, even though they were not differentially expressed. Therefore, we tested the concentration of retinoic acid in every group by ELISA. The results showed that compared with the normal group, the level of retinoic acid was lower in model group (P<0.05), but in the FZHY-treated group, the level was increased (P<0.05) (Figure 8F). We further performed a correlation analysis between three key genes' expression levels and retinoic acid production and the results showed that the expression trends of the genes and retinoic acid were consistent, although there was no statistically significant correlation (Supplementary Table S1).

Discussion

Liver fibrosis is the pathological consequence of chronic liver disease. An excessive deposition of ECM proteins occurs concomitantly with the processes of repair and regeneration[26, 27], leading to different degrees of loss of structure and function in the liver[28]. To prevent the development of liver disease, it is necessary to control or reverse fibrosis, but no effective treatment method is currently available for this condition[8]. At present, the treatment of fibrosis is focused on improving survival and quality of life and reducing the need for liver transplantation[28]. Recent studies showed that FZHY was effective in preventing liver fibrosis without adverse effects[8, 29], but the molecular mechanisms underlying these anti-fibrotic effects are not fully understood. Because system biology and network pharmacology have been widely applied in CHF studies, we analyzed and predicted potential targets and molecular mechanisms underlying the anti-fibrotic effects of FZHY using network pharmacological technologies based on the integrative analysis of transcriptomics and proteomics data.

Previous reports showed that CCl_4 induced liver inflammation

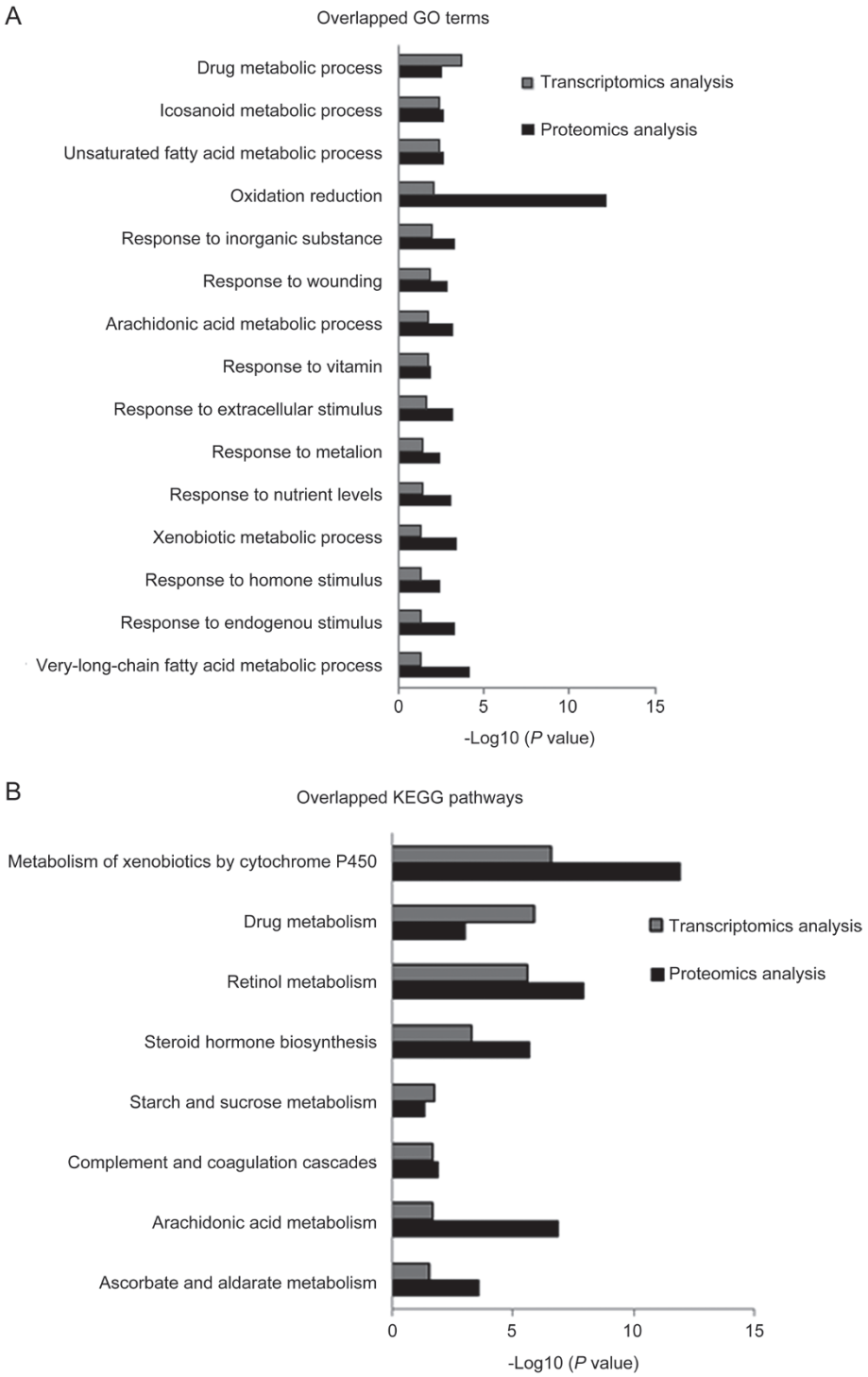

Figure 5. Overlapped GO terms and KEGG pathways in the FZHY-treated group. Gray pillar, GO terms or pathways by transcriptomic analysis; black pillar, GO terms or pathways by proteomic analysis.

and fibrosis in rat models[30, 31]. In this study, the levels of ALT, AST, TNF-α and IL-6 were significantly increased in the model group compared to the normal group. Our pathological findings from H&E staining showed increased inflammatory cell infiltration and Hyp content in the model group. Sirius Red staining did not show a fibrous septum in the normal group. We also performed qPCR to evaluate the expression levels of fibrosis-related genes, including α-SMA, collagen I and fibronectin. Compared to the model group, rats in the FZHY-treated group displayed significantly decreased levels of ALT, AST, TNF-α, IL-6, α-SMA, collagen I, fibronectin and Hyp content. The pathological findings suggested lower levels of inflammatory cells

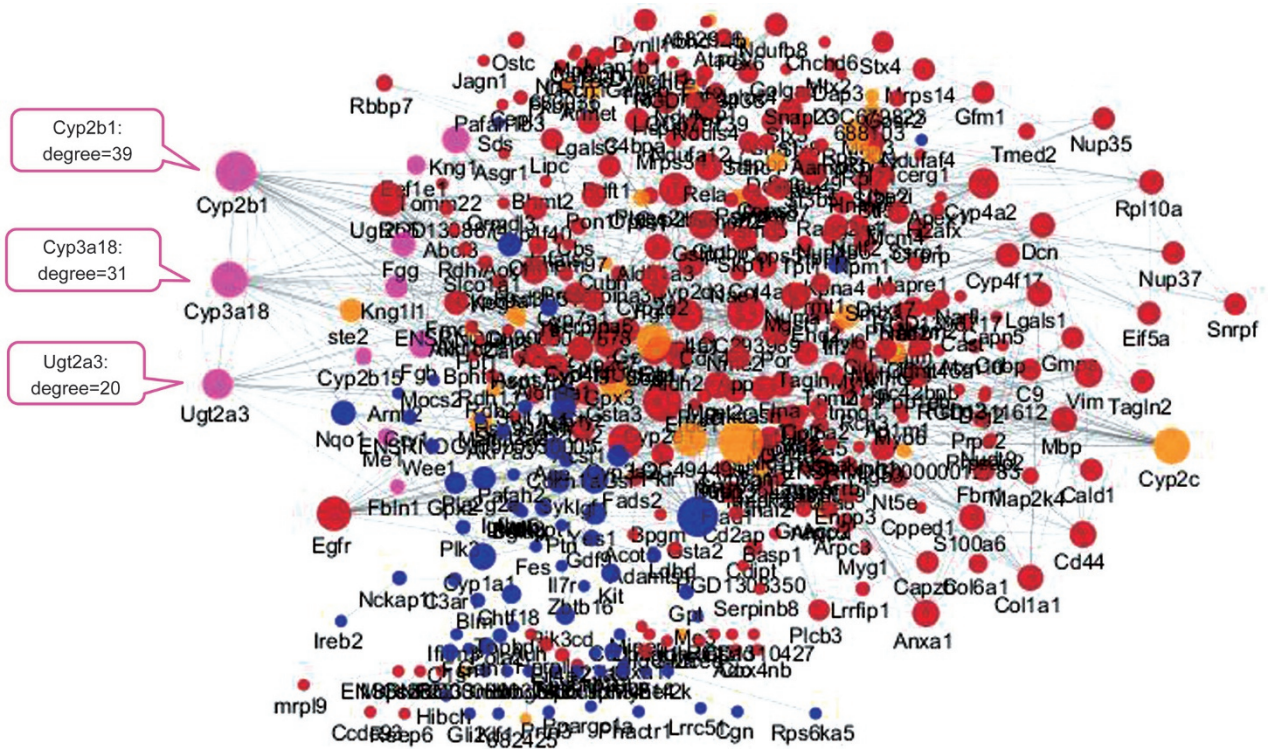

Figure 6. PPI network of the mechanisms underlying the anti-fibrotic effects of FZHY. The node color represents the degree of DEG and DEP co-expression. There were 10 nodes of overlapped DEG and DEP co-expression and higher degrees of overlap in the nodes of Ugt2a3 (20), Cyp2b1 (39), and Cyp3a18 (31). Red node, DEPs; blue node, DEGs; pink node, overlapped DEGs and DEPs; yellow node, the proteins in the STRING database.

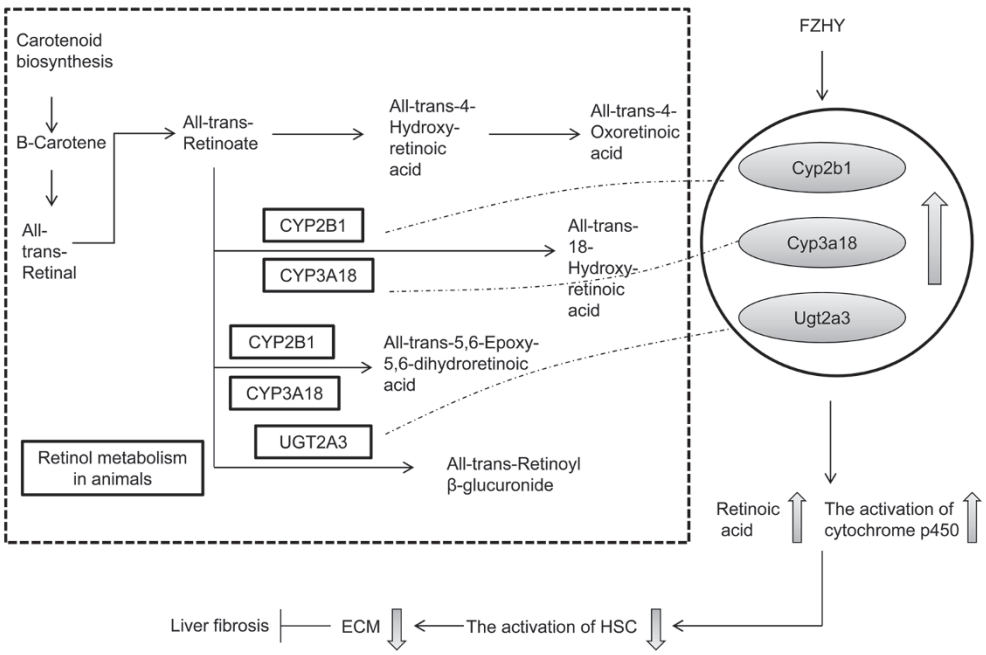

Figure 7. FZHY up-regulated Ugt2a3, Cyp2b1, and Cyp3a18 in the retinol metabolism pathway.

and fibrous septa (Figure 1 and 2). These results were consistent with other studies[32] and indicated that FZHY treatment can improve liver function, alleviate inflammation, decrease ECM deposition and attenuate pathological fibrotic changes in CCl_4-induced liver fibrosis in rats.

Our analysis was consistent with the research of others[33] and our previous study[34]. According to the integrative analysis of transcriptomics and proteomics data, 255 DEGs were

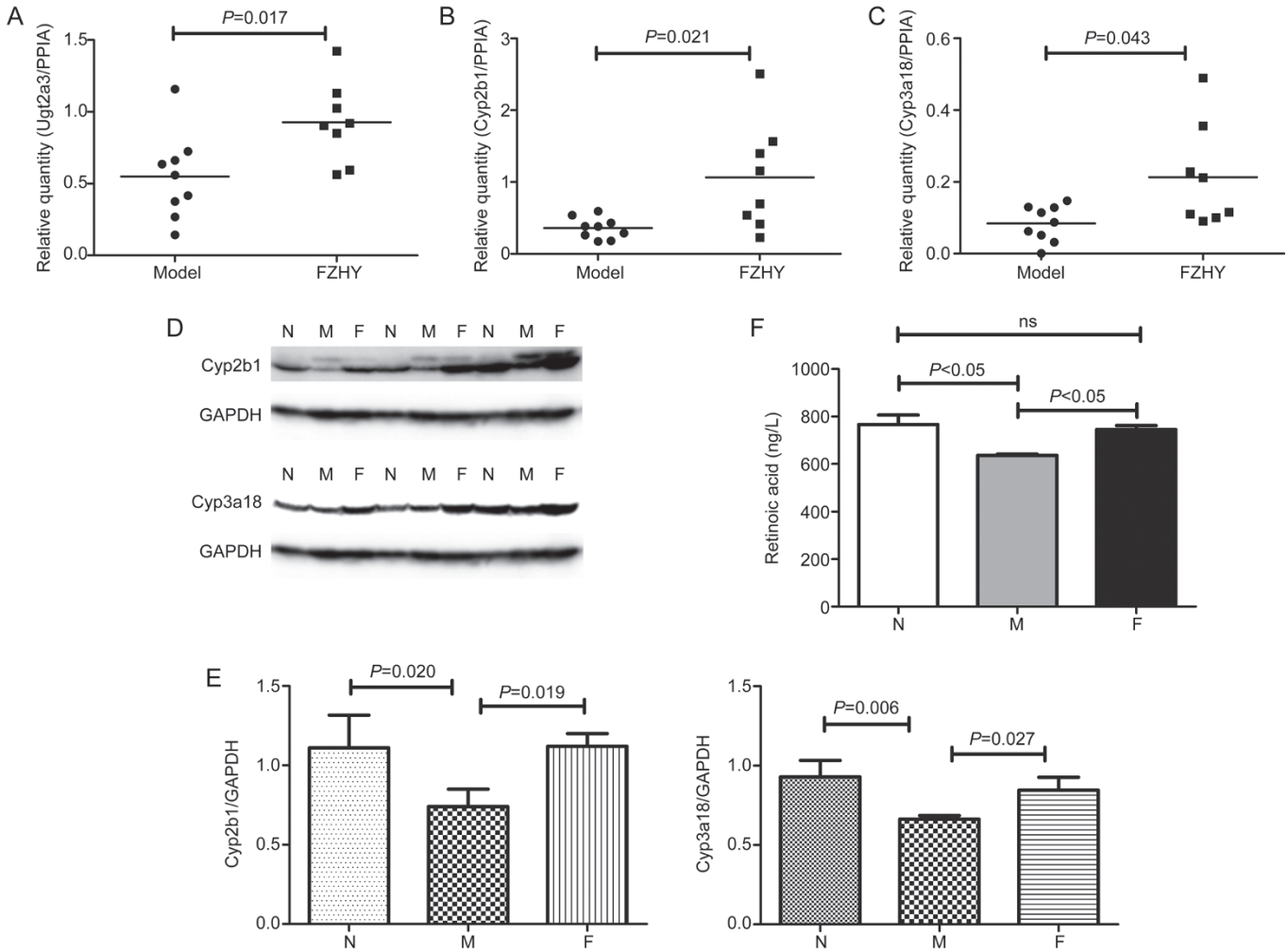

Figure 8. Expression levels of Ugt2a3, Cyp2b1, and Cyp3a18 by qRT-PCR and Western blot and the concentration of retinoic acid. Ugt2a3, Cyp2b1, Cyp3a18 and retinoic acid were all elevated in the FZHY-treated group compared to the model group. (A-C) qRT-PCR. (D) Western blot. (E) A quantity analysis was performed to demonstrate relative quantities in liver tissues. Mean±SD, *n*=8 or 9 in qRT-PCR; *n*=3 in Western blot. (F) Concentration of retinoic acid. The data are shown as mean±SEM, *n*=5.

enriched in 55 GO terms, 499 DEPs were enriched in 126 GO terms, and 15 GO terms overlapped (Figure 3 and 4). Apart from the aspects of the drug metabolic process, the anti-fibrotic biological processes of FZHY were predominantly related to oxidative stress, the inflammatory response, and ECM organization. Oxidative stress plays an important role in the pathogenesis of liver fibrosis through the activation of hepatic stellate cells[35, 36], resulting in weight loss, hepatocellular damage, disrupted cellular function[37], and hepatocyte death and regeneration[38]. Furthermore, oxidative stress leads to the release of pro-inflammatory and pro-fibrogenic cytokines that increase the synthesis of ECM components through the activation of quiescent HSCs[39]. Our analysis showed that FZHY down-regulate MDA levels, but there are no statistically significant differences in MDA and SOD levels between FZHY treatment and model groups, indicated that FZHY has not improved observably the oxidative stress in this study.

Moreover, we found that nine enriched pathways overlapped. These were mainly related to the regulation of metabolism, including the metabolism of xenobiotics by cytochrome P450, retinol metabolism, drug metabolism, starch and sucrose metabolism, arachidonic acid metabolism, and ascorbate and aldarate metabolism (Figure 4). Among these, retinol metabolism may play an important role in the anti-fibrotic effect of FZHY (Figure 5). Retinol and its derivative, retinoic acid, are critical to liver regeneration and pathogenesis, including inflammation, steatosis, fibrosis, and cirrhosis[40]. Retinol, cellular retinoic acid binding proteins, and retinol-metabolizing enzymes are stored in HSCs, the major producers of the fibrotic matrix[41, 42]. When the liver is exposed to CCl_4, which causes hepatocellular damage, HSCs are activated and retinol metabolism is impaired[43], resulting in liver fibrosis and cirrhosis[44], indicating that the regulation of retinol metabolism is one of the metabolism-related regulatory mechanisms involved in the effects of FZHY in the treatment of liver fibrosis. Furthermore, we found that the overlap of

Ugt2a3, Cyp2b1, and Cyp3a18 in the integrative analysis and co-expression in the PPI network (Figure 6) involved retinol metabolism, metabolism of xenobiotics by cytochrome P450, and drug metabolism (Figure 5) and validated that the expression levels of Ugt2a3, Cyp2b1, and Cyp3a18 were significantly increased in the FZHY-treated rats compared to the model rats at both the gene and protein levels (Figure 7). In a previous study, Ugt2a3, Cyp2b1, and Cyp3a18 were found to be involved in the generation of different kinds of retinoic acid, which ameliorated liver fibrosis[45], by inhibiting type I collagen expression and inflammation and by reducing oxidative stress in the liver[46]. This indicates that the increased expression of Ugt2a3, Cyp2b1, and Cyp3a18 would facilitate retinol metabolism to produce more retinoic acid (Figure 5). In fact, in the FZHY-treated group, we found higher retinoic acid levels compared with the model group (Figure 8F). Retinoic acid worked to suppress liver fibrosis[47], suggesting that the mechanisms underlying the anti-fibrotic effects of FZHY may be partly related to an increase in retinoic acid due to the up-regulated expression levels of Ugt2a3, Cyp2b1, and Cyp3a18.

In this study, we investigated the mechanisms of FZHY against liver fibrosis from the perspective of network pharmacology and there are some aspects that we need to improve in our subsequent study. First, the clinical data and samples need to be researched to support our findings. Second, the mechanisms we mentioned in this study should be verified by further investigation.

Conclusion

The anti-fibrotic effects of FZHY have been investigated previously, but the underlying mechanisms have not been fully elucidated. In this study, we investigated the molecular mechanisms underlying the anti-fibrotic effects of FZHY at the whole transcriptome and proteome levels. The results indicated that FZHY improved inflammation and fibrosis in a rat liver fibrosis model and that the underlying mechanisms involved the regulation of multiple targets, multiple functions, and multiple pathways, including improving oxidative stress, the inflammatory response, and ECM organization and regulating multiple metabolic pathways, such as retinol metabolism, metabolism of xenobiotics by cytochrome P450, and drug metabolism. Treatment with FZHY resulted in increased Ugt2a3, Cyp2b1, and Cyp3a18 expression levels, which may also play an important role in the anti-fibrotic effects of FZHY.

Acknowledgements

This work was supported by Key Program of National Natural Science Foundation of China (81330084), National Science and Technology Major Project of China (2009ZX09311-003), Shanghai Municipal Science and Technology Commission Project (12401900401), and E-institutes of Shanghai Municipal Education Commission (E03008).

Author contribution

Shi-bing SU, Yi-yang HU and Ping LIU conceived the research; Ya-nan SONG, Yang SUN, Bin WEI and Xiao-yan LI conducted the animal experiments; Shu DONG and Fei-fei CAI conducted the molecular assays and other experiments; Shu DONG and Qi-long CHEN performed the analysis; Shu DONG wrote the paper and Shi-bing SU revised the paper.

Supplementary information

Supplementary Table S1 is available on the website of Acta Pharmacologica Sinica.

References

1 Su TH, Kao JH, Liu CJ. Molecular mechanism and treatment of viral hepatitis-related liver fibrosis. Int J Mol Sci 2014; 15: 10578–604.
2 Sebastiani G, Gkouvatsos K, Pantopoulos K. Chronic hepatitis C and liver fibrosis. World J Gastroenterol 2014; 20: 11033–53.
3 Czaja AJ. Hepatic inflammation and progressive liver fibrosis in chronic liver disease. World J Gastroenterol 2014; 20: 2515–32.
4 Elpek GÖ. Cellular and molecular mechanisms in the pathogenesis of liver fibrosis: An update. World J Gastroenterol 2014; 20: 7260–76.
5 Dong S, Su SB. Advances in mesenchymal stem cells combined with traditional Chinese medicine therapy for liver fibrosis. J Integr Med 2014; 12: 147–55.
6 Zhao CQ, Wu YQ, Xu LM. Curative effects of Fuzheng Huayu capsules on hepatic fibrosis and the functional mechanisms: a review. Zhong Xi Yi Jie He Xue Bao 2006; 4: 467–72.
7 Dong S, Chen QL, Feng Q, Hu YY, Liu P, Su SB. Study of molecular mechanism of Fuzheng-Huayu Formula improved rats liver fibrosis based on analysis of gene expression profile. China J Tradit Chin Med Pharm 2015; 30: 1812–7.
8 Dong S, Chen QL, Su SB. Curative effects of Fuzheng Huayu on liver fibrosis and cirrhosis: a meta-analysis. Evid Based Complement Alternat Med 2015; 2015: 125659.
9 Liu C, Jiang CM, Liu CH, Liu P, Hu YY. Effect of Fuzheng Huayu decoction on vascular endothelial growth factor secretion in hepatic stellate cells. Hepatobiliary Pancreat Dis Int 2002; 1: 207–10.
10 Wang QL, Tao YY, Shen L, Cui HY, Liu CH. Chinese herbal medicine Fuzheng Huayu recipe inhibits liver fibrosis by mediating the transforming growth factor-β1/Smads signaling pathway. Zhong Xi Yi Jie He Xue Bao 2012; 10: 561–8.
11 Wang Q, Du H, Li M, Li Y, Liu S, Gao P, *et al*. MAPK signal transduction pathway regulation: a novel mechanism of rat HSC-T6 cell apoptosis induced by FUZHENGHUAYU tablet. Evid Based Complement Alternat Med 2013; 2013: 368103.
12 Li H, Zhao L, Zhang B, Jiang Y, Wang X, Guo Y, *et al*. A network pharmacology approach to determine active compounds and action mechanisms of ge-gen-qin-lian decoction for treatment of type 2 diabetes. Evid Based Complement Alternat Med 2014; 2014: 495840.
13 Zhang GB, Li QY, Chen QL, Su SB. Network pharmacology: a new approach for Chinese herbal medicine research. Evid Based Complement Alternat Med 2013; 2013: 621423.
14 Cheng L, Pan GF, Zhang XD, Wang JL, Wang WD, Zhang JY, *et al*. Yindanxinnaotong, a Chinese compound medicine, synergistically attenuates atherosclerosis progress. Sci Rep 2015; 5: 12333.
15 Shi SH, Cai YP, Cai XJ, Zheng XY, Cao DS, Ye FQ, *et al*. A network pharmacology approach to understanding the mechanisms of action of traditional medicine: Bushenhuoxue formula for treatment of chronic kidney disease. PLoS One 2014; 9: e89123.
16 Li X, Wu L, Liu W, Jin Y, Chen Q, Wang L, *et al*. A network pharmacology study of Chinese medicine QiShenYiQi to reveal its underlying multi-compound, multi-target, multi-pathway mode of

action. PLoS One 2014; 9: e95004.
17 An L, Feng F. Network pharmacology-based antioxidant effect study of zhi-zi-da-huang decoction for alcoholic liver disease. Evid Based Complement Alternat Med 2015; 2015: 492470.
18 Tang F, Tang Q, Tian Y, Fan Q, Huang Y, Tan X. Network pharmacology-based prediction of the active ingredients and potential targets of Mahuang Fuzi Xixin decoction for application to allergic rhinitis. J Ethnopharmacol 2015; 176: 402–12.
19 Zhang GB, Song YN, Chen QL, Dong S, Lu YY, Su MY, *et al*. Actions of Huangqi decoction against rat liver fibrosis: a gene expression profiling analysis. Chin Med 2015; 10: 39.
20 Song YN, Dong S, Wei B, Liu P, Zhang YY, Su SB. Metabolomic mechanisms of gypenoside against liver fibrosis in rats: An integrative analysis of proteomics and metabolomics data. PLoS One 2017; 12: e0173598.
21 Wang RQ, Mi HM, Li H, Zhao SX, Jia YH, Nan YM. Modulation of IKKβ/NF-κB and TGF-β1/Smad via Fuzheng Huayu recipe involves in prevention of nutritional steatohepatitis and fibrosis in mice. Iran J Basic Med Sci 2015; 18: 404–11.
22 Liu C, Liu P, Liu CH, Zhu XQ, Ji G. Effects of Fuzhenghuayu decoction on collagen synthesis of cultured hepatic stellate cells, hepatocytes and fibroblasts in rats. World J Gastroenterol 1998; 4: 548–9.
23 Lykkedegn S, Sorensen GL, Beck-Nielsen SS, Pilecki B, Duelund L, Marcussen N, *et al*. Vitamin D depletion in pregnancy decreases survival time, oxygen saturation, lung weight and body weight in preterm rat offspring. PLoS One 2016; 11: e0155203.
24 Pandit JJ, Handy JM. Science, Anaesthesia and animal studies: what is 'evidence'? Anaesthesia 2010; 65: 223–6.
25 Watanabe T, Suzuki T, Natsume M, Nakajima M, Narumi K, Hamada S, *et al*. Discrimination of genotoxic and non-genotoxic hepatocarcinogens by statistical analysis based on gene expression profiling in the mouse liver as determined by quantitative real-time PCR. Mutat Res 2012; 747: 164–75.
26 Crosas-Molist E, Fabregat I. Role of NADPH oxidases in the redox biology of liver fibrosis. Redox Biol 2015; 6: 106–11.
27 Lurie Y, Webb M, Cytter-Kuint R, Shteingart S, Lederkremer GZ. Non-invasive diagnosis of liver fibrosis and cirrhosis. World J Gastroenterol 2015; 21: 11567–83.
28 Crossan C, Tsochatzis EA, Longworth L, Gurusamy K, Davidson B, Rodríguez-Perálvarez M, *et al*. Cost-effectiveness of non-invasive methods for assessment and monitoring of liver fibrosis and cirrhosis in patients with chronic liver disease: systematic review and economic evaluation. Health Technol Assess 2015; 19: 1–409, v–vi.
29 Liu P, Hu YY, Liu C, Xu LM, Liu CH, Sun KW, *et al*. Multicenter clinical study on Fuzhenghuayu capsule against liver fibrosis due to chronic hepatitis B. World J Gastroenterol 2005; 11: 2892–9.
30 Abdel-Moneim AM, Al-Kahtani MA, El-Kersh MA, Al-Omair MA. Free radical-scavenging, anti-inflammatory/anti-fibrotic and hepatoprotective actions of taurine and silymarin against CCl_4 induced rat liver damage. PLoS One 2015; 10: e0144509.
31 Ogaly HA, Eltablawy NA, El-Behairy AM, El-Hindi H, Abd-Elsalam RM. Hepatocyte growth factor mediates the antifibrogenic action of *Ocimum bacilicum* essential oil against CCl_4-induced liver fibrosis in rats. Molecules 2015; 20: 13518–35.
32 Sun S, Dai J, Wang W, Cao H, Fang J, Hu YY, *et al*. Metabonomic evaluation of ZHENG differentiation and treatment by Fuzhenghuayu tablet in hepatitis-B-caused cirrhosis. Evid Based Complement Alternat Med 2012; 2012: 453503.
33 Ippolito DL, AbdulHameed MD, Tawa GJ, Baer CE, Permenter MG, McDyre BC, *et al*. Gene expression patterns associated with histopathology in toxic liver fibrosis. Toxicol Sci 2016; 149: 67–88.
34 Dong S, Chen QL, Song YN, Sun Y, Wei B, Li XY, *et al*. Mechanisms of CCl_4-induced liver fibrosis with combined transcriptomic and proteomic analysis. J Toxicol Sci 2016; 41: 561–72.
35 Mohamed Suhaimi NA, Zhuo L. Imidazolium salt attenuates thioacetamide-induced liver fibrosis in mice by modulating inflammation and oxidative stress. Dig Liver Dis 2012; 44: 665–73.
36 He W, Shi F, Zhou ZW, Li B, Zhang K, Zhang X, *et al*. A bioinformatic and mechanistic study elicits the antifibrotic effect of ursolic acid through the attenuation of oxidative stress with the involvement of ERK, PI3K/Akt, and p38 MAPK signaling pathways in human hepatic stellate cells and rat liver. Drug Des Devel Ther 2015; 9: 3989–4104.
37 Domitrović R, Jakovac H, Marchesi VV, Blažeković B. Resolution of liver fibrosis by isoquinoline alkaloid berberine in CCl_4-intoxicated mice is mediated by suppression of oxidative stress and upregulation of MMP-2 expression. J Med Food 2013; 16: 518–28.
38 Di Maso V, Mediavilla MG, Vascotto C, Lupo F, Baccarani U, Avellini C, *et al*. Transcriptional up-regulation of APE1/Ref-1 in hepatic tumor: role in hepatocytes resistance to oxidative stress and apoptosis. PLoS One 2015; 10: e0143289.
39 Teraoka R, Shimada T, Aburada M. The molecular mechanisms of the hepatoprotective effect of gomisin A against oxidative stress and inflammatory response in rats with carbon tetrachloride-induced acute liver injury. Biol Pharm Bull 2012; 35: 171–7.
40 Park S, Choi S, Lee MG, Lim C, Oh J. Retinol binding protein-albumin domain III fusion protein deactivates hepatic stellate cells. Mol Cell 2012; 34: 517–22.
41 Yi SH, Zhang Y, Tang D, Zhu L. Mechanical force and tensile strain activated hepatic stellate cells and inhibited retinol metabolism. Biotechnol Lett 2015; 37: 1141–52.
42 Miyazaki H, Takitani K, Koh M, Inoue A, Kishi K, Tamai H. Retinol status and expression of retinol-related proteins in methionine-choline deficient rats. J Nutr Sci Vitaminol (Tokyo) 2014; 60: 78–85.
43 De Paula TP, Ramalho A, Braulio VB. The effectiveness of relative dose response to retinol intake as an evaluation of vitamin A status of cirrhotic patients. J Hum Nutr Diet 2010; 23: 583–9.
44 Chang WT, Ker CG, Hung HC, Lee KT, Chen LS, Chiang HC, *et al*. Albumin and prealbumin may predict retinol status in patients with liver cirrhosis. Hepatogastroenterology 2008; 55: 1681–5.
45 Hisamori S, Tabata C, Kadokawa Y, Okoshi K, Tabata R, Mori A, *et al*. All-trans-retinoic acid ameliorates carbon tetrachloride-induced liver fibrosis in mice through modulating cytokine production. Liver Int 2008; 28: 1217–25.
46 Wang L, Potter JJ, Rennie-Tankersley L, Novitskiy G, Sipes J, Mezey E. Effects of retinoic acid on the development of liver fibrosis produced by carbon tetrachloride in mice. Biochem Biophys Acta 2007; 1772: 66–71.
47 Panebianco C, Oben JA, Vinciguerra M, Pazienza V. Senescence in hepatic stellate cells as a mechanism of liver fibrosis reversal: a putative synergy between retinoic acid and PPAR-gamma signalings. Clin Exp Med 2017; 17: 269–80.